

Performance of supersonic model combustors with staged injections of supercritical aviation kerosene

Feng-Quan Zhong · Xue-Jun Fan · Gong Yu ·
Jian-Guo Li · Chih-Jen Sung

Received: 3 September 2009 / Revised: 16 April 2010 / Accepted: 4 May 2010 / Published online: 21 July 2010
© The Chinese Society of Theoretical and Applied Mechanics and Springer-Verlag GmbH 2010

Abstract Supersonic model combustors using two-stage injections of supercritical kerosene were experimentally investigated in both Mach 2.5 and 3.0 model combustors with stagnation temperatures of approximately 1,750 K. Supercritical kerosene of approximately 760 K was prepared and injected in the overall equivalence ratio range of 0.5–1.46. Two pairs of integrated injector/flameholder cavity modules in tandem were used to facilitate fuel-air mixing and stable combustion. For single-stage fuel injection at an upstream location, it was found that the boundary layer separation could propagate into the isolator with increasing fuel equivalence ratio due to excessive local heat release, which in turns changed the entry airflow conditions. Moving the fuel injection to a further downstream location could alleviate the problem, while it would result in a decrease in combustion efficiency due to shorter fuel residence time. With two-stage fuel injections the overall combustor performance was shown to be improved and kerosene injections at fuel rich conditions could be reached without the upstream propagation of the boundary layer separation into the isolator. Furthermore, effects of the entry Mach number and pilot hydrogen on combustion performance were also studied.

Keywords Supersonic combustion · Staged injection · Combustion efficiency · Supercritical kerosene

The project was supported by the National Natural Science Foundation of China (10672169, 10621202).

F.-Q. Zhong · X.-J. Fan (✉) · G. Yu · J.-G. Li
LHD, Institute of Mechanics, Chinese Academy of Sciences,
100190 Beijing, China
e-mail: xfan@imech.ac.cn

C.-J. Sung
University of Connecticut, Storrs, CT 06269, USA

1 Introduction

In hydrocarbon-fueled scramjet operations, the onboard fuel will also be used as a coolant and its temperature and state will vary in different flight stages. When both fuel temperature and pressure are higher than the thermodynamic critical point, the fuel becomes supercritical, and supercritical fuel exhibits liquid-like density and gas-like diffusivity [1]. During injection the supercritical fuel can be directly transformed to the gaseous state without atomization and vaporization processes. Our previous experimental investigation [2] demonstrated that the use of supercritical kerosene injection has the potential of enhancing fuel-air mixing and promoting overall burning intensity. In comparison with liquid fuel injections at similar fuel flow rates, experimental results [2, 3] in a Mach 2.5 model combustor showed that the static pressure rise in the combustor with supercritical fuel injection increased by 10–15% at equivalence ratios below 0.5. However, the advantage of supercritical fuel injection has not been fully exploited with the single-stage injection. Especially, further increase in the fuel flow rate and the pressure rise with single-stage injection was limited by the upstream propagation of boundary layer separation due to excessive heat release [4].

In order to suppress the upstream propagation of the boundary layer separation at higher fuel equivalence ratios, either a longer isolator or a further downstream injection location could be used. A longer isolator may cause an increase in drag and engine weight, while moving the injection location to further downstream may cause a decrease in combustion efficiency and lower pressure rise due to the shorter residence time for reactions. The concept of staged fuel injection [5–8] utilizes dispersed heat release to avoid locally excessive pressure rise occurring in the case of single-stage fuel injection at high equivalence ratios. As such, better pressure distributions

and higher thrust can be attained in a staged supersonic combustor [5–8]. In a practical scramjet operation, it is also advantageous to use proper fuel distributions to adjust the fuel delivery in accord with different flight conditions and achieve an optimum engine performance.

It is worth noting that the advantage of using staged fuel injections is not limited to the suppression of boundary layer separation only. The combustion of an upstream-injected fuel can provide an environment of large radical pool and high turbulent intensity for the downstream-injected fuel, thereby improving fuel/air mixing and enhancing burning efficiency. To further explore the potential of using a staged supersonic combustor combined with supercritical fuel injection, a series of experiments were conducted to characterize the combustion of supercritical kerosene injected at two different stages in both Mach 2.5 and 3.0 model combustors. Kerosene was injected through two pairs of integrated injector/flameholder cavity modules installed in tandem along the flow path. The effects of fuel injection location, combustor entry Mach number, and pilot hydrogen on the combustor performance were investigated and discussed in this experimental study.

2 Experimental specifications

2.1 Test facility

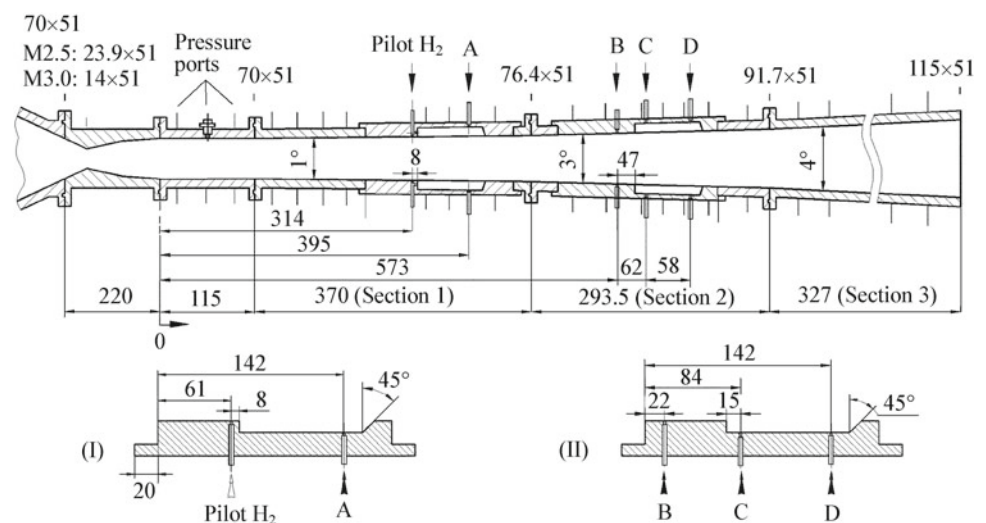
The experiments were conducted in a direct-connect wind tunnel facility, which consisted of a vitiated air supply system, a multi-purpose supersonic model combustor, and a kerosene delivery and heating system. The facility operation, control, and data acquisition were accomplished with a computer. The vitiated air heater, burning with H_2 , O_2 and N_2 , was used to supply heated airflow with a stagnation temperature of $T_0 = 1,750 \pm 70$ K. Different convergent-divergent nozzles were used to accelerate the flow to Mach 2.5 or

3.0. For comparison, the static pressure at the combustor entrance was kept almost identical for the two Mach numbers. As such, the corresponding stagnation pressures were set to $P_0 = 1.12 \pm 0.02$ and 2.44 ± 0.06 MPa for the Mach 2.5 and 3.0 flows, respectively. The stagnation pressure and temperature of the vitiated air were measured using a CYB-10S pressure transducer and a Type-B thermocouple, respectively.

The model combustor is shown in Fig. 1. It had a total length of 1,105.5 mm and consisted of one nearly constant area section of 115 mm and three divergent sections of 370 mm, 293.5 and 327 mm with the expansion angles of 1° , 3° and 4° , respectively. The entry cross section of the combustor was 70 mm in height and 51 mm in width. In Fig. 1, the “0” indicated at the beginning of the constant area section represents the origin for all the static pressure distributions to be presented and discussed later.

Two pairs of integrated fuel injector/flameholder cavity modules in tandem were installed on both sides of the combustor, each cavity with a depth of 12 mm, a 45° aft ramp angle, and an overall length-to-depth ratio of 7.3. There were four rows of wall injectors for kerosene injection, designated as Stages A–D in Fig. 1, corresponding to streamwise locations of 395, 573, 635 and 693 mm, respectively. Each row of injectors consisted of nine orifices of 1.0 mm in diameter evenly spaced in the spanwise direction and orientated normal to the wall surface. A small amount of pilot hydrogen was used to facilitate the self-ignition of kerosene in the supersonic combustor. There were five orifices of 1.0 mm in diameter available for the pilot hydrogen injection. Room temperature pilot hydrogen was injected normally to the airflow just upstream of the first pair of cavities, specifically at the streamwise location of 314 mm. The typical equivalence ratio of pilot hydrogen used in this study was 0.09. Distribution of the static pressure in the axial direction was determined using Motorola MPX2200 pressure transducers installed along the centerline of the model combustor

Fig. 1 Schematic of the Mach 2.5/3.0 model combustor (*top*) and configurations of two integrated fuel injection/flameholder modules (*bottom*). All length dimensions are in mm



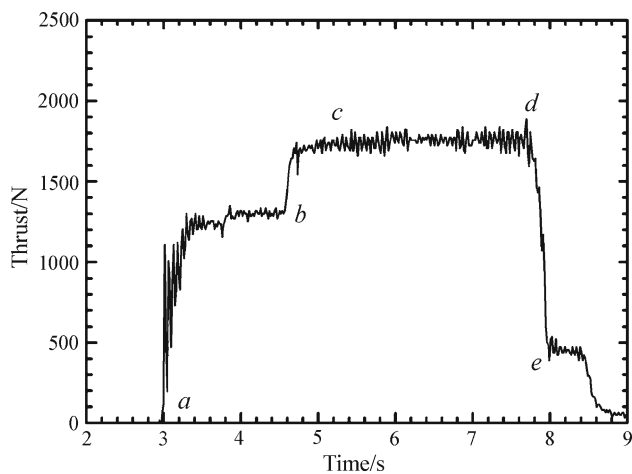


Fig. 2 Time history of thrust value during an experiment

sidewalls. The experimental uncertainty in the static pressure measurements was approximately 3%.

The entire test rig was mounted upright on a platform. Three weight sensors (Shanghai TM, Model No. NS-TH3), equilaterally spaced and connected in series, were used to support the platform and to measure the thrust changes during the experiments. This system yielded a maximum force reading of 7,500 N with an uncertainty of 0.2%. Figure 2 shows a typical result of time history of the thrust signal for a single run. The airflow started up at the point “a”. Subsequently, the thrust was seen to increase rapidly and level off within 1 s. Fuel injection then began at the point “b”.

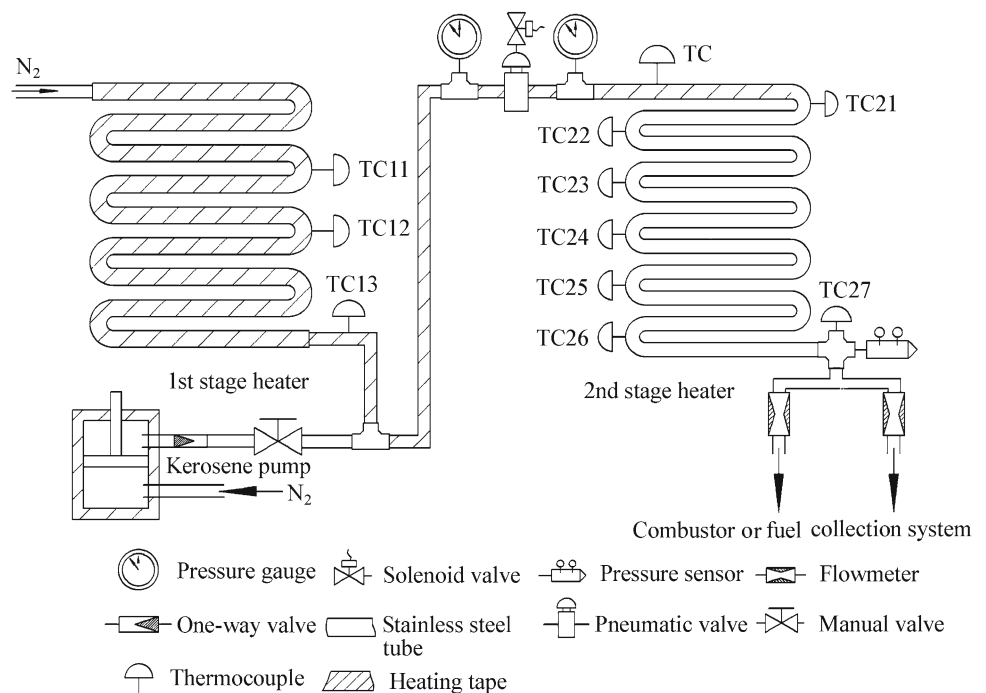
The thrust level further increased due to the fuel injection and the subsequent combustion, and quickly stabilized at the point “c”. After a certain experimental duration, the flows of H₂ and O₂ in the vitiated air heater and the fuel injection in the combustor were shut off at the point “d”, and hence the thrust quickly dropped to the point “e”. The residual thrust reading beyond the point “e” was due to the purge N₂ flow.

The nearly constant thrust level between the points “c” and “d” shown in Fig. 2 demonstrates the steadiness of the supersonic combustion and the adequacy of the present test facility. The thrust increment as a result of fuel injection and combustion is then defined as the thrust increase from the value at the point “b” to the average value between the points “c” and “d”. This thrust increment will be later used as one target parameter for the combustor performance assessment.

2.2 Kerosene delivery and heating system

Supercritical kerosene at temperature of 750 ± 20 K was prepared under varying pressures using the two-stage kerosene heating and delivery system developed in Ref. [2]. A schematic of this system is shown in Fig. 3. The first-stage heater was a storage type that can heat kerosene of 0.8 kg up to 570 K with negligible coking deposits and the second-stage heater was a continuous type, which was capable of rapidly heating kerosene to 750 K within a few seconds.

Fig. 3 Schematic of kerosene delivery and heating system



Prior to each experiment, the kerosene in a storage cylinder was pumped into the first-stage heater by a piston driven by high-pressure nitrogen gas. Two pneumatic valves (Swagelok, Model No. SS6UM and SS10UM) installed, respectively, at the exits of the first- and second-stage heaters were employed to turn on/off the two heaters sequentially. When kerosene in the first-stage heater reached a desired temperature at a given pressure, it was pressed into the second-stage heater and heated up to the working temperature before injected into the model combustor.

Two groups of K-type thermocouples (Omega, Model No. KMQSS-0.032E), denoted as TC11–13 and TC21–27 in Fig. 3, were installed on the surface of or inserted into the heater tubes. These thermocouples were used to monitor the fuel temperature distribution along the heating system and achieve the feedback control of the heating system. Stable fuel temperature and pressure at the exit of the heating system were accomplished and maintained during each experiment.

The mass flow rates of the supercritical kerosene were controlled and measured by sonic nozzles. The associated calibration procedure has been documented elsewhere [2]. In the cases of two-stage fuel injections, two sonic nozzles of different throat diameters were installed in parallel at the exit of the second-stage heater, as shown in Fig. 3. The mass flow rate of each sonic nozzle was determined based on the fuel temperature and pressure measured just upstream the nozzles. Considering the measurement accuracies of throat area, fuel pressure, and fuel temperature, the overall uncertainty associated with the measured fuel mass flow rate was within 5%.

3 Results and discussion

3.1 Single-stage fuel injection: effect of equivalence ratio on combustor performance

Experiments were first conducted in the Mach 2.5 combustor with single-stage fuel injection (at Stage A) under approximately identical airflow conditions: a stagnation temperature of $T_0 = 1,750 \pm 70$ K, a stagnation pressure of $P_0 = 1.12 \pm 0.02$ MPa, and a mass flow rate of $q = 1,200 \pm 20$ g/s. The kerosene was injected at the supercritical conditions of $T_f = 750 \pm 20$ K and $P_f = 4.0\text{--}4.98$ MPa. As such, the fuel mass flow rate varied from approximately 41–114 g/s, and the corresponding kerosene equivalence ratios were in the range of $\phi_f = 0.52\text{--}1.43$.

Figure 4 compares the measured static pressure distributions along the combustor for different fuel equivalence ratios. The case of “no combustion” (i.e. no fuel injection) was also plotted in Fig. 4 as a reference. It is seen from Fig. 4 that the overall pressure level increases with increasing equivalence ratio. Moreover, for $\phi_f > 0.6$ the pressure

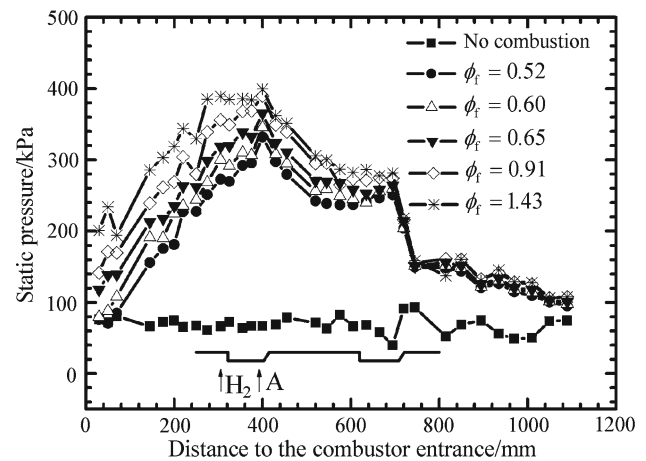


Fig. 4 Static pressure distributions with single-stage fuel injection at different fuel equivalence ratios. Vitiated Mach 2.5 air: $T_0 \approx 1,750$ K and $P_0 \approx 1.12$ MPa

rise began to propagate upstream out of the isolator and into the divergent section of the supersonic nozzle due to the separation of boundary layer caused by locally excessive heat release and shock-boundary layer interaction. As a result, the entry conditions (such as Mach number) of the combustor are expected to be changed, which should be avoided because it would cause an engine un-start.

Table 1 lists the measured values of specific thrust increment (Γ), defined as the thrust increments per unit mass flow rate of air, for the conditions of Fig. 4 as well as all other experiments conducted herein. Figure 5 plots the results corresponding to Fig. 4, showing the dependence of Γ on fuel equivalence ratio. The specific thrust increment is seen to increase with increasing kerosene equivalence ratio up to 0.9 and then become nearly constant for ϕ_f beyond 0.9.

3.2 Single-stage fuel injection: effect of fuel injection location on combustor performance

To avoid the combustion-induced pressure rise propagating upstream out of the isolator, experiments with single-stage fuel injection at different locations were carried out in the same Mach 2.5 combustor. The airflow and kerosene conditions were kept approximately identical to those used in Fig. 4. Two kerosene mass flow rates of 71 ± 2 g/s and 114 ± 2 g/s were tested, which correspond to the kerosene equivalence ratios of $\phi_f = 0.9 \pm 0.02$ and 1.44 ± 0.02 , respectively.

Figure 6 compares the static pressure distributions in the Mach 2.5 model combustor with four different kerosene injection locations (Stages A–D) for $\phi_f \approx 0.9$. Although the same amount of kerosene was injected at each location, the overall pressure rise with the Stage A injection was much higher than the other three injection cases. As the injection stage was moved to the downstream location, the overall pressure level decreased. It is also noted that the

Table 1 Experimental conditions and measured thrust increments per unit air mass flow rate

Figure	Vitiated air				Kerosene			Injector location	$\Gamma/(m \cdot s^{-1})$	
	P_0/MPa	T_0/K	M	$q/(\text{g} \cdot \text{s}^{-1})$	P_f/MPa	T_f/K	ϕ_f or ϕ_1/ϕ_2			
4	1.12	1,720	2.5	1,213	4.00	774	0.52	A	242	
	1.13	1,775		1,204	4.56	767	0.60		297	
	1.13	1,746		1,214	4.98	767	0.65		322	
	1.12	1,779		1,191	4.93	768	0.91		370	
6	1.11	1,759	2.5	1,190	4.94	758	1.43	A	369	
	1.12	1,779		1,191	4.93	768	0.91		370	
	1.13	1,760		1,214	4.88	762	0.90		B	347
	1.13	1,781		1,202	4.91	763	0.90		C	310
7	1.13	1,730	2.5	1,204	4.87	770	0.89	D	285	
	1.11	1,759		1,190	4.94	758	1.43		A	369
	1.13	1,765		1,209	4.95	748	1.44		B	312
	1.14	1,820		1,200	4.90	731	1.46		C	312
8	1.13	1,837	2.5	1,184	4.96	742	1.44	D	343	
	1.13	1,736		1,218	5.03	763	0.51/0.37		A+B	330
	1.13	1,742		1,216	5.07	756	0.52/0.38		A+C	348
	1.14	1,795		1,207	5.15	777	0.51/0.37		A+D	351
10	2.45	1,801	3.0	1,475	4.58	755	1.05	A	363	
	2.43	1,791		1,466	4.53	763	1.03		B	299
	2.50	1,822		1,495	4.52	760	1.00		C	250
	2.43	1,764		1,477	4.52	746	1.04		D	220
11	2.50	1,884	3.0	1,465	4.10	750	0.46/0.62	A+B	344	
	2.38	1,721		1,471	4.13	761	0.45/0.61		A+C	298
	2.44	1,766		1,486	4.12	757	0.45/0.61		A+D	296

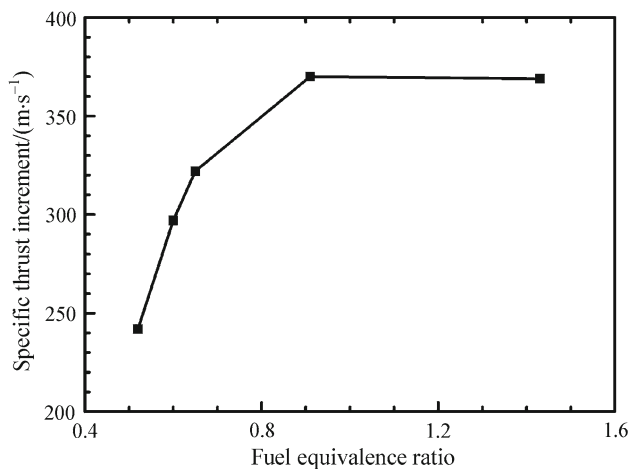


Fig. 5 Specific thrust increment as a function of fuel equivalence ratio for the conditions of Fig. 4

pressure downstream of the second cavity module increased slightly when changing the injection location from Stage A to Stage D.

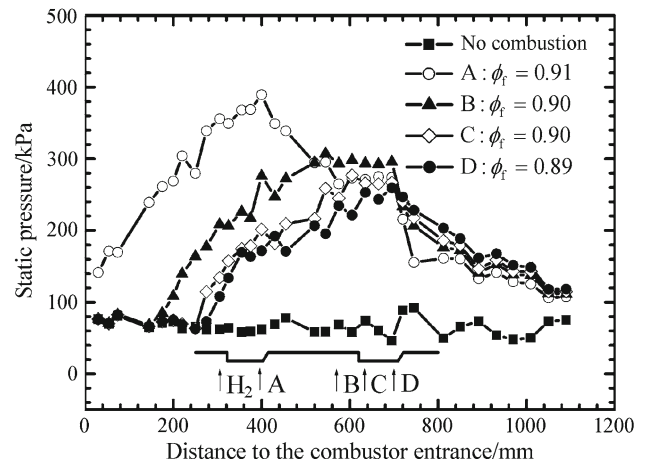


Fig. 6 Comparison of static pressure distributions with single-stage fuel injection at four different locations for fuel equivalence ratio of $\phi_f \approx 0.9$. Vitiated Mach 2.5 air: $T_0 \approx 1,750$ K and $P_0 \approx 1.12$ MPa

The thrust increment decreased from 370 to 285 m/s when the injection location was moved from Stage A to Stage D. It can be explained by the fact that as the injection location

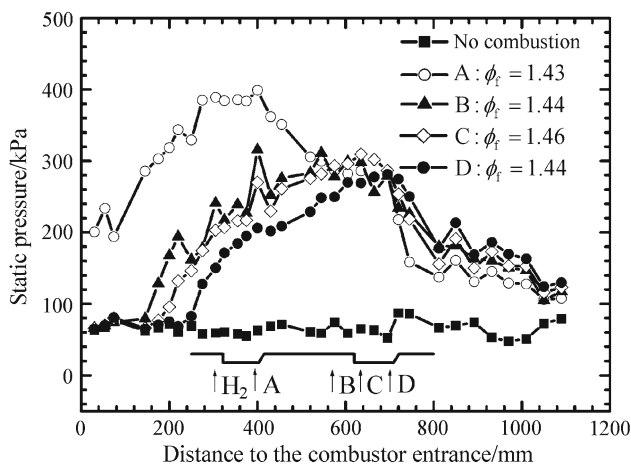


Fig. 7 Comparison of static pressure distributions with single-staged fuel injection at four different locations for fuel equivalence ratio of $\phi_f \approx 1.44$. Vitiated Mach 2.5 air: $T_0 \approx 1,750$ K and $P_0 \approx 1.12$ MPa

moves downstream, the residence time available for fuel-air mixing and the subsequent combustion became more limited.

Figure 7 shows and compares the pressure distributions for single-stage fuel injection at a higher fuel equivalence ratio of $\phi_f \approx 1.44$. The trend of static pressure distribution variation with different injection locations is seen to be similar to that shown in Fig. 6. As listed in Table 1, Γ decreased from 369 to 312 m/s when the injection location was moved from Stage A to Stage C, but increased to 343 m/s for Stage D injection even with much lower pressure rise in the first half section of the combustor. It appears that for Stage D injection, the higher pressure rise downstream of the second cavity module where the divergent angle of the combustor was the largest accounted for the increase in Γ .

3.3 Effect of two-staged fuel injection on combustor performance

To circumvent the pressure rise propagating out of the isolator and simultaneously maintain a relatively high specific thrust increment, two-stage fuel injections were tested in the present supersonic model combustor, by keeping the total fuel mass flow rate constant as used in Fig. 6. The first-stage injection was at the location of Stage A with 57.5% of the total kerosene mass flow rate, while the remaining 42.5% was injected through one of the other three stages. As such, the overall kerosene equivalence ratios at the first and second stages were $\phi_1 \approx 0.52$ and $\phi_2 \approx 0.38$. Figure 8 compares the static pressure distributions with the three injection combinations, namely A+B, A+C, and A+D. It is of interest to see from Fig. 8 that the static pressure profiles for all three two-stage injection combinations were very similar, although some small variations occurred near the entrance of the combustor. The differences in the specific thrust increments for

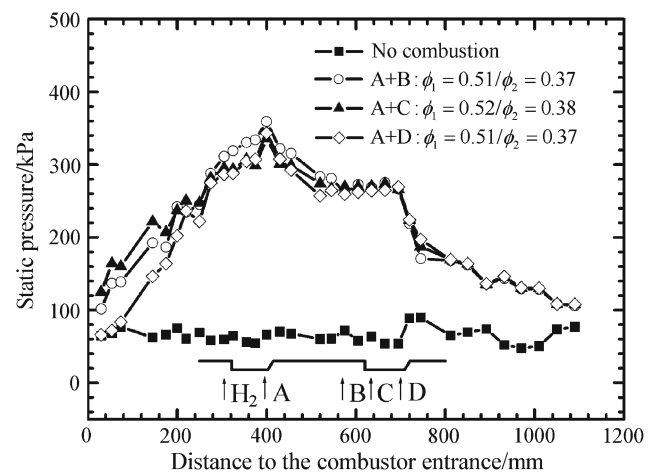


Fig. 8 Comparison of static pressure distributions using three different combinations of two-stage fuel injections with constant total fuel mass flow rate. Vitiated Mach 2.5 air: $T_0 \approx 1,750$ K and $P_0 \approx 1.12$ MPa

all three combinations were also very small, as shown in Table 1. Compared to the single-stage injection cases shown in Fig. 6, Γ of the A+B combination (330 m/s) was slightly smaller than that of Stage B single injection (347 m/s), while Γ 's of the A+C and A+D combinations (348 and 351 m/s, respectively) were significantly larger than those of Stage C (310 m/s) and Stage D (285 m/s) single injections. This comparison therefore demonstrates the potential of two-stage injections in enhancing the fuel-air mixing and the overall burning intensity. Such an enhancement could be attributed to several factors, including the availability of radical pools, the changes in local Mach number, and the increase in turbulence intensity resulting from the burning of the fuel injected at the first stage.

Further experiments were conducted to examine the effects of varying the fuel injection ratio between the first and second stages, by keeping the conditions of airflow and total kerosene mass flow rate nearly the same as those used in Figs. 6 and 8. Sonic nozzles with different throat diameters were used to distribute the two-stage fuel injections, which allowed systematic variations in ϕ_1 and ϕ_2 while fixing $\phi_1 + \phi_2$ approximately constant at 0.90. The measured specific thrust increments were then plotted against $\phi_2/(\phi_1 + \phi_2)$. Figure 9 summarizes the test results using the two-stage injection combinations of A+B and A+D. Within the current experimental uncertainty, Γ is seen to generally decrease with increasing portion of the second-stage injection for the injection combination of A+D, while first decrease and then increase for the injection combination of A+B as $\phi_2/(\phi_1 + \phi_2)$ was increased. Hence, it suggests that for the purpose of thrust optimization, as much fuel as possible should be injected at the upstream stage as long as there is no combustion pressure propagating out of the isolator.

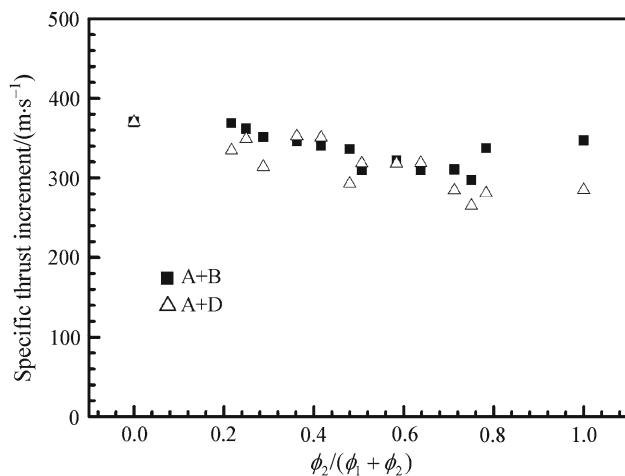


Fig. 9 Specific thrust increments as a function of $\phi_2/(\phi_1 + \phi_2)$ for the two-stage injection combinations of A+B and A+D

3.4 Effect of entry mach number on combustor performance

The combustor entry Mach number plays an important role in affecting the combustor performance. A higher entry Mach number would reduce the overall burning intensity due to shorter combustor residence time, particularly with fuel injected at locations closer to the combustor exit. To verify the effectiveness of staged injections on performance enhancement with a higher entry Mach number, a series of experiments with single- and two-stage kerosene injections were also carried out in a Mach 3.0 model combustor under the following airflow conditions: a stagnation temperature of $1,750 \pm 70$ K, a stagnation pressure of 2.45 ± 0.03 MPa, and a mass flow rate of $1,480 \pm 20$ g/s. The kerosene was injected at the supercritical conditions of 750 ± 20 K and 4.55 ± 0.03 MPa. The total kerosene mass flow rate was 103 ± 2 g/s, corresponding to an overall equivalence ratio of 1.03 ± 0.03 .

Figure 10 shows the single-stage injection results by comparing the static pressure distributions along a Mach 3.0 combustor with fuel injected at four different locations of A–D. In comparison with the Mach 2.5 test results shown in Fig. 6, although the trend in pressure level variations with different injection locations is similar, larger disparity in static pressure distributions between injection locations of B–D is noted. Particularly, Fig. 10 shows very low burning intensity for the Stage D injection case, in which most of injected fuel left the combustor without combustion. Compared to the Mach 2.5 cases, Table 1 further demonstrates that the specific thrust increments of the Mach 3.0 cases decreased significantly for fuel injections at Stage B–D but remained approximately the same for Stage A injection. As discussed earlier, a higher flow speed reduces the fuel residence time

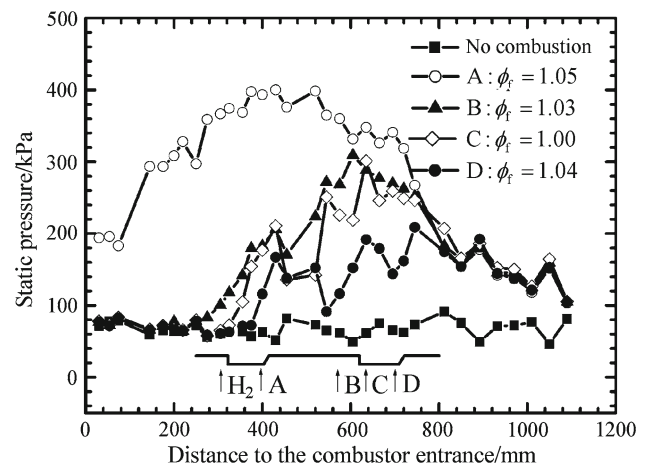


Fig. 10 Comparison of static pressure distributions with single-stage fuel injections at four different locations under similar fuel injection conditions. Vitiated Mach 3.0 air: $T_0 \approx 1,750$ K and $P_0 \approx 2.45$ MPa

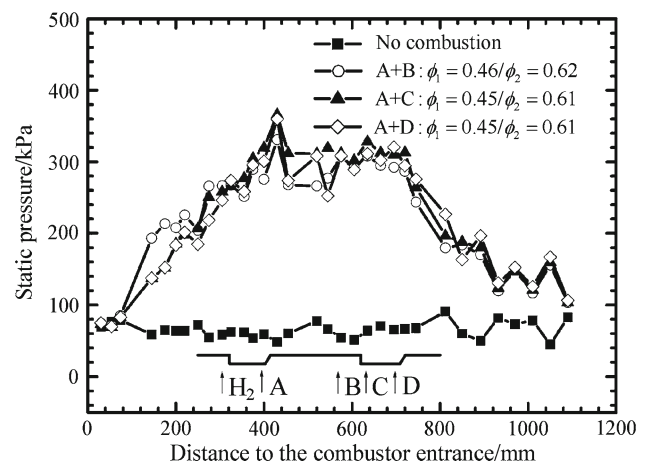


Fig. 11 Comparison of static pressure distributions with two-stage fuel injections under similar fuel injection conditions. Vitiated Mach 3.0 air: $T_0 \approx 1,750$ K and $P_0 \approx 2.45$ MPa

inside the combustor, leading to lower level of fuel-air mixing and less extent of complete combustion.

Figure 11 compares the static pressure profiles for the three injection combinations of A+B, A+C, and A+D in the present Mach 3.0 combustor. Approximately 42.5% of the total fuel mass flow rate was injected through Stage A and the remaining 57.5% was injected through one of the three stages B–D located at the second cavity module. Figure 11 shows that the static pressure profiles for all three combinations were fairly similar. It can also be seen from Table 1 that the specific thrust increments for all two-stage injections increased significantly as compared to the single-stage injections at the downstream locations of B, C and D. Comparison of thrust increment with staged injection for Mach 2.5 and Mach 3 combustors shows that staged injection is more beneficial for higher Mach number flow.

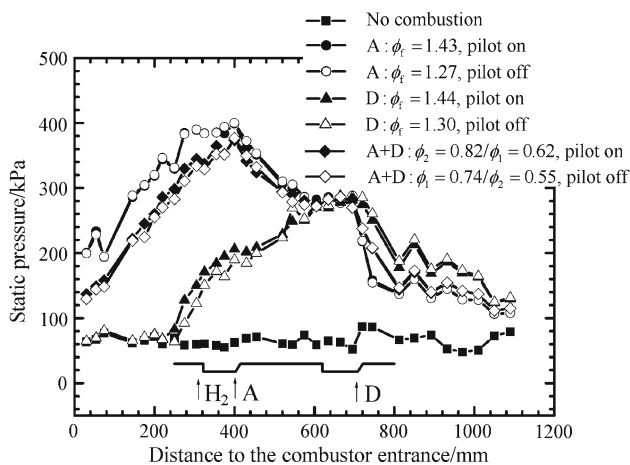


Fig. 12 Comparison of static pressure distributions with and without pilot hydrogen injections. Vitiated Mach 2.5 air: $T_0 \approx 1,750$ K and $P_0 \approx 1.12$ MPa

3.5 Effect of pilot hydrogen

The preceding experimental results were obtained with the help of pilot hydrogen at an equivalence ratio of 0.09. To clarify the role of pilot hydrogen in the cases with two-stage fuel injections, the pilot hydrogen during the experiments was turned off about one second earlier than kerosene. Thus, the combustor performances with and without pilot hydrogen can be assessed. Figure 12 compares the static pressure distributions in our Mach 2.5 model combustor with fuel injections at Stage A, Stage D, and the combination of A+D, with and without pilot hydrogen injection. The airflow and fuel injection conditions were kept nearly identical to those used in Fig. 7. When the pilot hydrogen was turned off, it is seen from Fig. 12 that stable combustion was still maintained in all cases investigated. Moreover, the overall pressure level was almost not affected for Stage A injection, and decreased only slightly for the cases with Stage D injection and the A+D injection combination. Similar effect of pilot hydrogen on combustor performance was also observed for the Mach 3.0 combustor, but the reduction in static pressure when the pilot hydrogen was turned off was slightly larger than that for the Mach 2.5 cases.

4 Conclusions

Combustor performances with single- and two-stage injections of supercritical kerosene were experimentally investigated and compared in both Mach 2.5 and 3.0 model combustors. Static pressure distributions within the combustor and thrust increments were measured and used to assess the combustor performance. The key results are summarized as follows.

With single-stage fuel injection, the increase in the fuel flow rate and the associated pressure rise were limited by the upstream propagation of boundary layer separation due to excessive local heat release. Although moving the fuel injection location to downstream could suppress the upstream propagation of boundary layer separation, it would result in lower thrust increment due to reduced fuel residence time. The use of two-stage injection was shown to be effective in the suppression of boundary layer separation as well as able to maintain relatively high levels of combustion pressure and thrust increment. Compared to the case with single-stage injection at a downstream location, the overall burning intensity was found to improve significantly by a combination of partial fuel injected at an upstream location with the rest injected further downstream.

Furthermore, it is found higher entry Mach number would result in lower levels of fuel-air mixing and burning intensity because of reduced fuel residence time, but the combustor performance could be improved significantly with two-stage fuel injections. The experiments also demonstrated that the effect of pilot hydrogen is minimal when stable combustion was established.

Acknowledgments The authors would like to acknowledge Prof. X. N. Lu for the assistance in designing and testing the kerosene heater. We also thank Mr. Y. Li and Mr. X. S. Wei for technical supports.

References

1. Yang, V.: Modeling of supercritical vaporization, mixing and combustion processes in liquid-fueled propulsion system. In: Proceeding of the Combustion Institute, **28**, 925–942 (2000)
2. Fan, X.J., Yu, G., Li, J.G., et al.: Investigation of vaporized kerosene injection and combustion in a supersonic model combustor. *J. Propuls. Power* **22**(1), 103–110 (2006)
3. Fan, X.J., Yu, G., Li, J.G., et al.: Combustion and ignition of thermally cracked kerosene in supercritical model combustors. *J. Propuls. Power* **23**(2), 317–324 (2007)
4. Billig, F.S., Dugger, G.L., Waltrap, P.J.: Inlet-combustor interface problem in scramjet engines. In: Proceeding of the International Symposium on Air Breathing Engines (1972)
5. Thomas, S.R., Guy, R.W.: Scramjet Testing from Mach 4–20—Present Capability and Needs for the Ninties. AIAA Paper 90-1388 (1990)
6. Vinogradov, V., Grachev, V., Petrov, M., et al.: Experimental investigation of 2-D Dual Mode Scramjet with Hydrogen Fuel at Mach 4–6, AIAA Paper 90-5269, (1990)
7. Tomioka, S., Murakami, A., Kudo, K., et al.: Combustion tests of a staged supersonic combustor with a strut. *J. Propuls. Power* **17**(2), 293–300 (2001)
8. Tomioka, S., Kobayashi, K., Kudo, K., et al.: Effects of injection configuration on performance of a staged supersonic combustor. *J. Propuls. Power* **19**(5), 876–884 (2003)